# A quantum ring terahertz detector with resonant tunnel barriers

G. Huang,[1] W. Guo,[1] P. Bhattacharya,[1,a)] G. Ariyawansa,[2] and A. G. U. Perera[2]
[1]*Department of Electrical Engineering and Computer Science, Solid State Electronics Laboratory, University of Michigan, Ann Arbor, Michigan 48109-2122, USA*
[2]*Department of Physics and Astronomy, Georgia State University, Atlanta, Georgia 30303, USA*

(Received 10 February 2009; accepted 26 February 2009; published online 13 March 2009)

The electronic properties of InAs/GaAs quantum rings and the characteristics of resonant tunnel intersubband terahertz detectors with quantum ring active regions have been studied. The electronic states of the quantum rings have been calculated and measured by the capacitance-voltage technique. The detectors exhibit extremely low dark current density values $\sim 5\times 10^{-5}$, $4.7\times 10^{-2}$, and $3.5\times 10^{-1}$ A/cm$^2$ under a $-1$ V bias at 4.2, 80, and 300 K, respectively. Three prominent response peaks are observed at $\sim$6.5, 10, and 12.5 THz up to $T=120$ K. At 80 K, the responsivity of the peaks varies from 0.07 to 0.02 A/W. © *2009 American Institute of Physics*. [DOI: 10.1063/1.3100407]

The generation and detection of terahertz (THz) radiation have gained importance for their potential applications in the areas of security, biomedical imaging, quality control, and submillimeter astronomy.[1–4] Various techniques and technologies are being explored for the realization of suitable terahertz detectors,[5,6] particularly ones that can detect in the 3–10 THz range and at high temperatures ($\geq$80 K). In particular, the use of intersublevel absorption in quantum dots (QDs) allows the detection of normally incident radiation. QD detectors in the 15–100 THz range have been demonstrated,[7] but it is difficult to access the 3–10 THz range. Another nanostructure of interest for this application is the quantum ring (QR), which can be formed after the epitaxy of self-organized InAs QDs on GaAs.[8] A few nanometers of a GaAs or GaAs/AlAs cap layers are grown on the pyramid/lens-shaped QD. The growth is then interrupted and an *in situ* anneal is performed. The QD transforms into a QR due to the lateral diffusion of indium. The height, inner diameter, and outer diameter of the rings are typically 2–4, 50, and 80 nm, respectively (see Fig. 1). There is some evidence that the confinement energies of these nanostructures are suitable for terahertz detection via intersublevel absorption.[9] In the present study we have investigated the electronic properties of InAs/GaAs QRs grown by molecular beam epitaxy (MBE) and have characterized tunnel QR intersubband detectors (QRIDs) that demonstrate absorption in the 3–8 THz range up to 80 K and at higher frequencies up to 120 K.

The electron energy levels of the QRs were calculated by solving the time-independent Schrödinger equation within the effective mass approximation. The ring was modeled as a 2 nm high hollow cylinder with inner and outer radii of 25 and 40 nm, respectively. Because most of the quantum confinement effects result from the 2 nm vertical dimension and much less from the third dimension (around the ring), as a further simplification, the ring was treated as a quantum wire with $15\times 2$ nm$^2$ rectangular cross-section. The resulting eigenvalue problem is solved numerically and the calculated energy levels in the QR are depicted in Fig. 1. Capacitance-voltage ($C$-$V$) measurements were made at 10 K to determine the spectral position of the bound electron and hole levels in the QRs. These measurements made with QD heterostructures have been described in detail by other authors.[10] The device heterostructure grown by MBE is schematically shown in Fig. 1. The QRs are embedded in an undoped GaAs matrix and are formed as follows. After growth of the GaAs tunneling barrier layer at 600 °C, the substrate temperature was lowered to 530 °C and 2.6 ML of InAs was deposited at a rate of 0.05 ML/s. Self-organized QDs were formed following growth of 1.8 ML of an InAs wetting layer. A 10 Å/10 Å GaAs/AlAs cap layer was grown on the InAs islands at 530 °C. Growth was interrupted and the capped islands were annealed at 560 °C for 1 min under an $As_2$ flux to form the QRs. Atomic force microscopy (AFM) imaging of exposed QR layers (Fig. 1) indicates that the aerial density of the rings is $\sim 10^{10}$ cm$^{-2}$. The rest of the heterostructure, starting with the 40 nm undoped GaAs spacer layer, was grown at a substrate temperature of 600 °C. Two heterostructures were grown, with $n$- and $p$-type back contact layers, for the measurement of electron and hole energy levels, respectively. The tunnel barrier layer thickness of the $p$-type sample was made smaller to account for the smaller tunneling rate of holes, compared to that of electrons, in GaAs. Diode structures having 640 $\mu$m diameter mesas with Cr/Au Schottky gates on top and appropriate alloyed back contacts were fabricated by standard optical lithography, wet etching, and metallization techniques. By

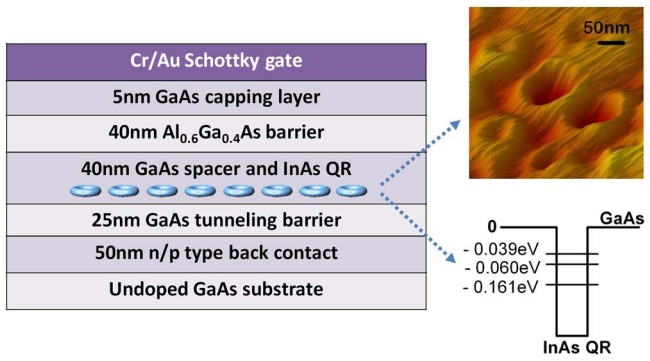


FIG. 1. (Color online) Schematic heterostructure of Schottky diode for capacitance-voltage measurements grown by MBE. Insets show AFM image of InAs QRs and calculated electron energy states.

a)Electronic mail: pkb@eecs.umich.edu.

 

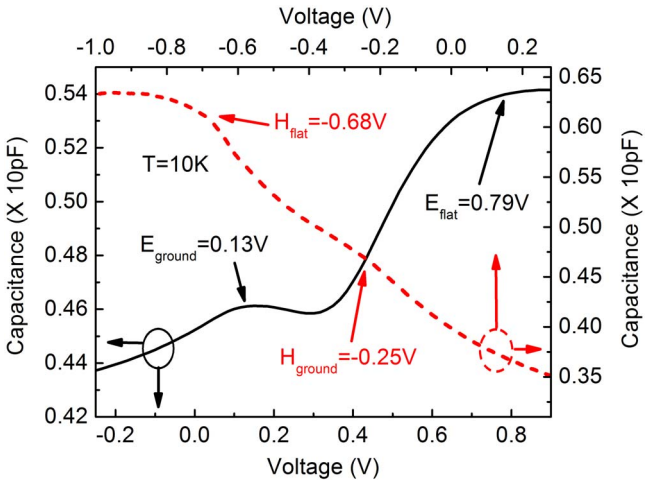


FIG. 2. (Color online) Capacitance-voltage measurement data from QR heterostructures. The electron and hole ground state energies obtained from the analysis of these data are in good agreement with calculated values.

changing the dc bias, the equilibrium Fermi level can be moved in energy inside the GaAs band gap and through all electron and hole quantized levels in the QRs. The measured capacitance is the sum of the geometric capacitance (inversely related to the sample thickness), the density-of-states capacitance, and a capacitance resulting form charge accumulation in different parts of the heterostructure. The measured *C-V* characteristics for the *n*- and *p*-type samples are shown in Fig. 2. The plateaus in the two cases correspond to carrier accumulation in the two-dimensional wetting layer, while the peaks labeled $E_{\text{ground}}$ and $H_{\text{ground}}$ are believed to originate from the electron and hole ground states of the QR. The calculated excited states of the QRs are not observed. The feature attributed to the hole ground state originates, in all probability, from a mixture of heavy-hole and light-hole states. From analysis of the measured data, the confinement energies of the electron and hole ground states, with respect to the GaAs band edges, are estimated to be 150 and 98 meV, respectively. The former is in reasonably good agreement with the calculated value quoted earlier.

A critical parameter in the operation of long-wavelength detectors is the dark current, which should be as small as possible to enhance the specific detectivity $D^*$. We have recently reported a tunneling QD infrared photodetector (QDIP) (Ref. 11) in which we have demonstrated a reduction in dark current by two orders of magnitude, compared to that in a detector without the tunneling heterostructure.[12] The conduction band profile of one period of the QR with the resonant tunneling structure and the complete heterostructure with 15 QR layers (to enhance absorption) and grown by MBE are shown in Fig. 3(a). The double barrier resonant tunneling heterostructure preferably transports the photoexcited electrons while blocking a significant fraction of the electrons (with an energy spread) that contribute to the dark current. The calculated electron energy levels in the QR are also indicated in the figure. The purpose of the $Al_{0.1}Ga_{0.9}As$ barrier on the side of the ring opposite to the tunnel barriers is to create a well and quasibound states within it, which will be resonant with the tunneling states in the $In_{0.2}Ga_{0.8}As/Al_{0.2}Ga_{0.8}As$ double barrier heterostructure. The energy levels in the quantum well are calculated by solving the one-dimensional Schrödinger equation including the

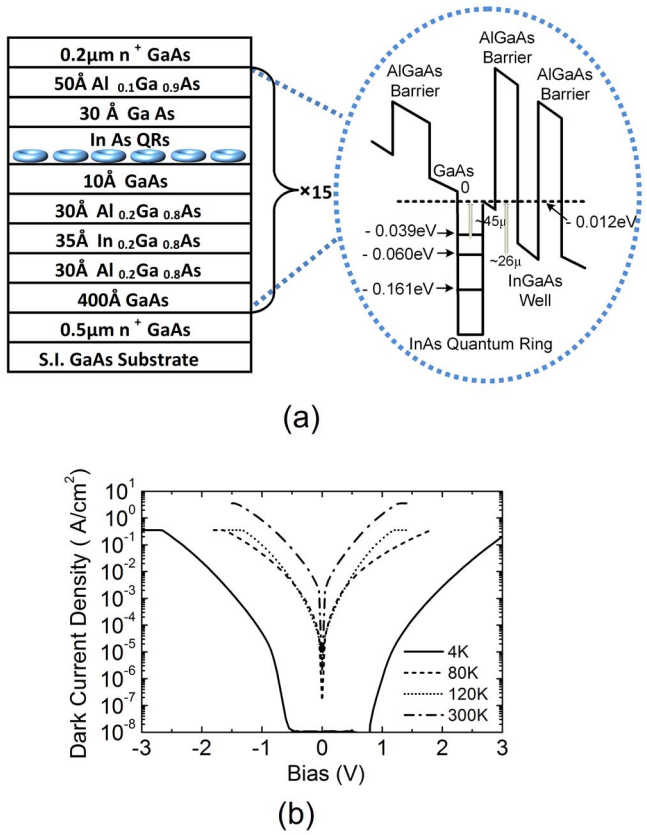


FIG. 3. (Color online) (a) Heterostructure schematic of QRID grown by MBE. The inset depicts one period of the QR layer together with double barrier resonant tunneling heterostructure. (b) Measured temperature-dependent dark current as a function of bias.

presence of the wetting layer. Tunability in the energy position of these energy levels is afforded by varying the height (composition) of the single AlGaAs barrier. Mesa-shaped devices for top illumination were fabricated by photolithography, wet chemical etching, and *n*-contact metallization. The ring-shaped top contact has an inner radius of 300 $\mu$m, which defines the illumination area.

The dark current-voltage characteristics in the temperature range of 4–300 K, measured with a Keithley 2400 Source Meter, are shown in Fig. 3(b). The dark currents are comparable to and as low as those measured in resonant tunneling QDIPs.[11] The current densities at a bias of $-1$ V are $5\times10^{-5}$, $4.7\times10^{-2}$, and $3.5\times10^{-1}$ A/cm$^2$ at 4.2, 80, and 300 K, respectively. The normal incidence spectral response was measured with a globar broadband source and a System 2000 Perkin Elmer Fourier transform infrared spectrometer. To calibrate the response, spectra of a Si composite bolometer, with a known sensitivity, were obtained with the same set of optical components. For this study we have focused in the spectral range of 20–100 $\mu$m (3–15 THz). The calibrated spectral response of the QRID devices at 5, 80, and 120 K with an applied bias of $-2$ V is shown in Fig. 4. It is apparent that the data indicate three responsivity peaks at ~6.5 THz (46 $\mu$m), 10 THz (30 $\mu$m), and 12.5 THz (24 $\mu$m). The longitudinal optical phonon absorption in GaAs and AlAs are seen as the resonances (dips) at ~8.3 THz (36 $\mu$m) and 11 THz (27 $\mu$m), respectively. These dips have been observed and reported in similar devices.[13–15] The peaks at 48 and 25 $\mu$m correspond extremely well with transitions originating from the two calcu-

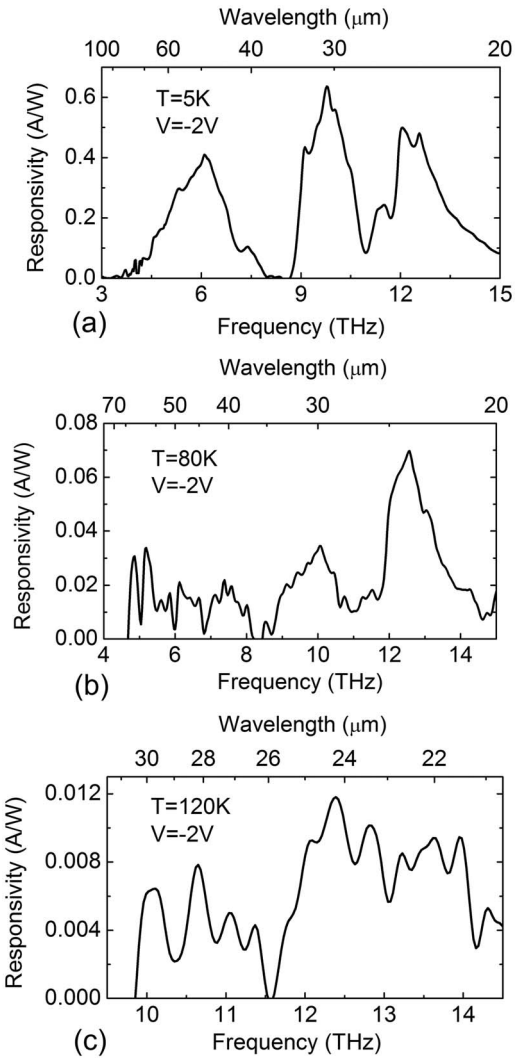


FIG. 4. Calibrated spectral responsivity of resonant tunneling QRIDs measured at (a) 5, (b) 80, and (c) 120 K.

lated QR excited states, shown in Fig. 3(a), to the quantum well/resonant tunneling state. The origin of the responsivity peak centered at 30 $\mu$m is not well understood at this time. One possibility is the existence of QRs of two sizes, which has been reported earlier.[16] A more likely explanation is the existence of additional confined states due to the nontrivial geometry of the QRs, which are not determined from the simple effective mass calculation. It may also be noted that the 46 $\mu$m transition is not observed in the 120 K measurement data, but the transitions at 24 and 30 $\mu$m are still present. In general, the transitions appear to be broad because they are at very long wavelengths. The width of the 46 $\mu$m peak at 5 K is only 7.5 meV. It is of interest to note that at 5 K, the peak responsivities corresponding to the three transitions are almost comparable though they are widely separated in wavelength. At 80 K, the peak amplitude decreases with increasing wavelength. At 120 K, the peak amplitudes of both observable transitions are weak. Generally, the peak responsivity in the terahertz range shows a decreasing trend with increasing temperature. There are two competing factors that determine the relative magnitude of the temperature-dependent responsivity of the different absorption peaks. For the same incident power, there are more photons at longer wavelengths. Also, with increase in temperature, the occupation of the higher excited states decreases by thermionic emission. Finally, the noise performance becomes a significant factor, although our tunnel filter helps to a large extent.

The QRID noise current was measured with a current preamplifier and fast Fourier transform signal analyzer. A thick copper plate was used to shield the device from outer radiation. The specific detectivity ($D^*$), a measure of the signal-to-noise ratio of the terahertz detector, was calculated from the noise density spectra and responsivity in accordance with the relation $D^*=R_pA^{1/2}/S_i^{1/2}$, where $A$ is the illumination area and $S_i$ is the noise density spectra. The values of $D^*$ for the 10 THz response peak at 5 and 80 K are $4.9\times10^9$ Jones and $9.5\times10^7$ Jones, respectively, at a bias of $-2$ V.

The work was supported by the Air Force Office of Scientific Research under Grant No. FA9550-06-1-0500 and the National Science Foundation under Grant No. ECS-0620688.

[1]Y. C. Shen, T. Lo, P. F. Taday, B. E. Cole, W. R. Tribe, and M. C. Kemp, Appl. Phys. Lett. **86**, 241116 (2005).
[2]P. H. Siegel, IEEE Trans. Microwave Theory Tech. **52**, 2438 (2004).
[3]C. Zandonella, Nature (London) **424**, 721 (2003).
[4]T. G. Phillips and J. Keene, Proc. IEEE **80**, 1662 (1992).
[5]H. C. Liu, C. Y. Song, A. J. SpringThorpe, and J. C. Cao, Appl. Phys. Lett. **84**, 4068 (2004).
[6]M. B. M. Rinzan, A. G. U. Perera, S. G. Matsik, H. C. Liu, Z. Wasilewski, and M. Buchanan, Appl. Phys. Lett. **86**, 071112 (2005).
[7]P. Bhattacharya, X. H. Su, S. Chakrabarti, G. Ariyawansa, and A. G. U. Perera, Appl. Phys. Lett. **86**, 191106 (2005).
[8]A. Lorke, R. J. Luyken, J. M. Garcia, and P. M. Petroff, Jpn. J. Appl. Phys., Part 1 **40**, 1857 (2001).
[9]J.-H. Dai, J.-H. Lee, Y.-L. Lin, and S.-C. Lee, Jpn. J. Appl. Phys. **47**, 2924 (2008).
[10]G. Medeiros-Ribeiro, D. Leonard, and P. M. Petroff, Appl. Phys. Lett. **66**, 1767 (1995).
[11]X. H. Su, S. Chakrabarti, P. Bhattacharya, G. Ariyawansa, and A. G. U. Perera, IEEE J. Quantum Electron. **41**, 974 (2005).
[12]X. H. Su, S. Chakrabarti, A. D. Stiff-Roberts, J. Singh, and P. Bhattacharya, Electron. Lett. **40**, 1082 (2004).
[13]H. Luo, H. C. Liu, C. Y. Song, and Z. R. Wasilewski, Appl. Phys. Lett. **86**, 231103 (2005).
[14]A. B. Weerasekara, M. B. M. Rinzan, S. G. Matsik, A. G. U. Perera, M. Buchanan, H. C. Liu, G. von Winckel, A. Stintz, and S. Krishna, Opt. Lett. **32**, 1335 (2007).
[15]J. C. Cao, Y. L. Chen, and H. C. Liu, Superlattices Microstruct. **40**, 119 (2006).
[16]G.-Z. Jia, J.-H. Yao, Y.-C. Shu, X.-D. Xing, and B. Pi, Appl. Surf. Sci. **255**, 4452 (2009).